J. Biochem. 2010;147(5):743–749 doi:10.1093/jb/mvq007

JB THE JOURNAL OF BIOCHEMISTRY

Kinetics of agonist-induced intrinsic fluorescence changes in the *Torpedo* acetylcholine receptor

Received September 8, 2009; accepted January 12, 2010; published online January 31, 2010

Hideki Kawai[1,*] and Michael A. Raftery[1,2,†]

[1]Department of Pharmacology, University of Minnesota Medical School, Minneapolis, MN 55455; and [2]Department of Biochemistry, University of Minnesota, St. Paul, MN 55108, USA

*Hideki Kawai, Department of Bioinformatics, Faculty of Engineering, Soka University, Hachiouji, Tokyo 192-8577, Japan, Tel: +81-42-691-9396, Fax: +81-42-691-9312, E-mail: kawai@soka.ac.jp

†In memory of Dr Michael A. Raftery.

The nicotinic acetylcholine receptor from *Torpedo* electric organs is a ligand-gated ion channel that undergoes conformational transitions for activation and/or desensitization. Earlier work suggested that intrinsic fluorescence changes of the receptor monitors kinetic transitions toward the high-affinity, desensitized state. Here, using highly purified membrane preparations to minimize contaminating fluorescence, we examined kinetic mechanisms of the receptor as monitored by its intrinsic fluorescence. Fluorescence changes were specific to the receptor as they were blocked by α-bungarotoxin and were induced by agonists, but not by the antagonist hexamethonium. Acetylcholine, carbamylcholine and suberyldicholine showed only one kinetic phase with relatively fast rates ($t_{1/2} = 0.2–1.2$ s). Effective dissociation constants were at least an order of magnitude higher than the high affinity, equilibrium binding constants for these agonists. A semirigid agonist isoarecolone-methiodide, whose activation constant was ~3-fold lower than acetylcholine, induced an additional slow phase ($t_{1/2} = 4.5–9$ s) with apparent rates that increased and then decreased in a concentration dependent manner, revealing a branched mechanism for conformational transitions. We propose that the intrinsic fluorescence changes of the receptor describe a process(es) toward a fast desensitization state prior to the formation of the high affinity state.

Keywords: acetylcholine/α-bungarotoxin/isoarecolone/nicotinic/receptor kinetics.

Abbreviations: ACh, acetylcholine; ANTS, 8-amino-1,3,6-naphthalene trisulfonic acid disodium salt; α-BTx, α-bungarotoxin; Carb, carbamylcholine; IAS, 5-(iodoacetamido)salicylate; Isoarecolone-MeI, isoarecolone-methiodide; nAChR, nicotinic acetylcholine receptor; SbCh, suberyldicholine.

The *Torpedo* nicotinic acetylcholine receptor (nAChR) is a pentameric ion channel composed of four homologous subunits—two α subunits and each of β, γ, δ subunits (*1*, *2*). It is generally agreed that, under equilibrium conditions, each receptor carries two high affinity binding sites at the interfaces formed by α–γ and α–δ subunits (*3–6*). Accumulating evidence indicates that, within the high affinity sites, there are two mutually exclusive, allosterically coupled, subsites that are ~15–20 Å apart depending on conformational states of the receptor (*7–12*). In addition to the high affinity sites, there is evidence for the presence of the low affinity agonist-specific sites, whose properties are consistent with their participation in receptor activation (*13–15*). Thus, the high affinity sites may involve in receptor function other than receptor activation.

Agonist binding to the receptor induces conformational changes to open the channel rapidly and to desensitize it more slowly (*16*). Understanding the mechanisms of conformational changes is fundamentally important, and, to this end, fluorescence changes that accompany agonist binding to the receptor have been useful to monitor kinetic behavior. Investigators have utilized non-covalent extrinsic fluorescent probes (*17–19*), fluorescent cholinergic ligands (*20–23*) and a covalently attached fluorescence probe (*10*, *14*, *15*, *24*) to detect conformational transitions of the receptor, but the rate constants were too slow to account for receptor activation and were attributed to desensitization processes. A protein that contains tryptophan residues in its primary sequence can be examined for conformational transitions by monitoring intrinsic fluorescence changes of the amino acid derived from alteration in the surrounding environment. The use of such intrinsic fluorescence was attempted with solubilized nAChR and membrane bound nAChR. Despite its relatively high quantum yield, the solubilized receptor did not produce a fluorescence change after mixing with various cholinergic ligands (*25*). Barrantes and his colleagues have used the membrane-bound nAChR from *Torpedo marmorata* and have been able to detect intrinsic fluorescence quenching of the receptor upon binding of cholinergic ligands (*26–28*). As was the case for extrinsic probes, the conformational transitions observed were slow and probably corresponded to a desensitization process(es).

Here, we have investigated the intrinsic fluorescence change induced by acetylcholine (ACh), carbamylcholine (Carb), suberyldicholine (SbCh) as well as isoarecolone-methiodide (isoarecolone-MeI)—an ACh analog with a dihydropyridine moiety between the

acetyl group and the quaternary amine (*29*). This semi-rigid ligand is a very potent agonist at the neuromuscular junction (*30*, *31*). In contrast to previous studies, the membrane preparations used were alkali-treated to remove auxiliary proteins (*32–34*), thus minimizing contaminating fluorescence. All agonists induced a kinetic phase with apparent rates about an order of magnitude greater than those previously reported (*26–28*) while the kinetics with isoarecolone-MeI contained an additional phase with a slow rate.

Materials and Methods

Materials

Carbamylcholine chloride and acetylcholine chloride were from Sigma Chemical Co. Suberyldicholine diiodide was from Aldrich. Hexamethonium chloride dihydrate was from Mann Research Laboratories (Orangeburg, NY); Isoarecolone-MeI was provided by Dr Charles E. Spivak (National Institute of Drug Abuse, Baltimore, MD). 8-amino-1,3,6-naphthalene trisulfonic acid disodium salt (ANTS) was from Invitrogen/Molecular Probes Inc.

nAChR-enriched membrane fragments were prepared from *Torpedo californica* (Aquatic Research Consultants, San Pedro, CA) as described previously (*34*). The concentration of the receptor was measured by a DEAE disc assay (*35*).

Thallium(I)-flux stopped-flow experiments

Membrane vesicles loaded with ANTS were prepared and Tl^+-flux stopped-flow experiments were conducted as described previously (*36*). Briefly, fast kinetic fluorescence quenching of ANTS following entry of Tl^+ into the vesicles was measured using an SF.17MV MicroVolume stopped-flow spectrofluorimeter apparatus (Applied Photophysics Ltd., Leatherhead, UK) with a xenon arc lamp (150 W) for excitation at 370 nm. Fluorescence traces were analyzed for rates and amplitudes using a modified Stern–Volmer equation:

$$F(t) = \frac{A_1}{1 + KT_\infty(1 - e^{-kt})} + k_0 t + A_0,$$

where $F(t)$ is the fluorescence intensity at time t, A_1 is the fluorescence intensity in the absence of Tl^+, K is a Stern–Volmer constant for a fluorophore, T_∞ is the maximum concentration of Tl^+ inside the vesicles, k is the apparent rate constant of Tl^+ flux, k_0 is the rate of Tl^+ leak through the membrane, A_0 is the fluorescence intensity fir the baseline. The concentration–rate curve was fitted with the sigmoidal equation:

$$\log\left[\frac{k_{app}}{k_{max} - k_{app}}\right] = n\log[L] - n\log K_{act},$$

where k_{app} is the apparent rate of fluorescence quenching at each ligand concentration, k_{max} is the maximum rate of quenching, n is the Hill coefficient, $[L]$ is the free ligand concentration and K_{act} is an apparent activation constant for channel opening.

Ligand-induced intrinsic fluorescence changes

Kinetic measurements of intrinsic fluorescence changes were conducted using the SF.17MV stopped-flow apparatus with excitation wavelength of 282 nm, and a bandpass filter was placed in the excitation beam to reduce stray light. Emission was recorded using a filter with 300 nm cutoff. An equal volume of the *Torpedo* membrane fragments and *Torpedo* Ringers buffer (20 mM HEPES, pH 7.4, 250 mM NaCl, 5 mM KCl, 4 mM $CaCl_2$, 2 mM $MgCl_2$, 0.02% NaN_3) with or without a ligand(s) were rapidly mixed to give a final receptor concentration of 20 nM (in α-BTx binding sites) throughout the experiments. Unless otherwise stated, each kinetic trace was fit with the following two exponential model equation:

$$F(t) = A_0 + A_f[\exp(-k_f t)] + A_s[\exp(-k_s t)] + k_0 t,$$

where $F(t)$ is the fluorescence level at time t, A_0 is the equilibrium fluorescence level, k_f and k_s are the apparent rates of the two processes, A_f and A_s are the amplitudes corresponding to the apparent rates, and k_0 is the slope of the base line to correct for photolysis effects. The Carb-induced kinetic traces in the absence or presence of various concentrations of hexamethonium were analyzed by assuming $A_s = 0$ (*i.e.* a single exponential model).

In order to enhance the resolution of biphasic kinetics, split time scales of 0.2 and 2 s (0.2/2 s), 2 and 20 s (2/20 s), and 10 s (or 5 s) and 50 s [10 (or 5)/50 s] were used. The rate constants for the 10 (or 5)/50 s time scale were similar to those of the 2/20 s time scale. The kinetic traces of the 0.2/2 s time scale could not be analyzed consistently and accurately since the initial 100 ms of the early signals contained random fluorescence changes in these time ranges. Overall, the kinetic traces obtained with 2/20 s time scale provided a good description of intrinsic fluorescence kinetics. For mechanism fitting, the rate constants for any phase in which the time scale of the reaction was <2.5 times or more than 25 times the half-life of that phase were excluded (*24*). Furthermore, since each split time contained 200 data points, rate constants whose half-life contained <15 data points were also eliminated. The apparent rate constants were averaged for each set of experiments and plotted as a function of ligand concentrations.

RESULTS

Kinetics and specificity of agonist-induced intrinsic fluorescence changes

Rapid mixing of membrane fragments and cholinergic agonists resulted in a time-dependent reduction of intrinsic fluorescence of the nAChR. The Carb-induced fluorescence change (Fig. 1A, trace b) was blocked by pretreatment of the membrane fragments with α-BTx (Fig. 1A, trace c), indicating the fluorescence change was specific for this agonist binding to the receptor. This specificity was further evidenced since the antagonist hexamethonium blocked the Carb-induced intrinsic fluorescence change in a concentration dependent manner with a half-maximal inhibition of 1.32 ± 0.29 mM (Fig. 1B). No significant intrinsic fluorescence change was observed with this antagonist alone. The components of the kinetic traces included a linear decrease in fluorescence, due to photolysis of the receptor protein as demonstrated by closing the excitation light path with a shutter and observing that the fluorescence level returned to the level prior to the shutter closing when it was reopened at later times.

Concentration dependent effects of acetylcholine, carbamylcholine and suberyldicholine

As demonstrated previously (*27*, *28*), ACh, Carb (data not shown), and SbCh (Fig. 2) induced a change in intrinsic fluorescence of the receptor protein and this effect was concentration dependent. The apparent rates for the fast phase were consistently observed for these ligands. However, slow rates were not obtained as observed for isoarecolone-MeI (see below); therefore, only the fast phase was considered for further analysis.

Assuming that (i) the fluorescence decrease reflects conformational transitions of the receptor upon binding of a ligand and that (ii) the binding of a ligand is rapid and diffusion controlled (*i.e.* $>10^8\ M^{-1}\ s^{-1}$), the following simple sequential mechanism was consistent with our observations:

Scheme I

$$R + L \underset{}{\overset{K_1}{\rightleftharpoons}} RL \underset{k_2}{\overset{k_2}{\rightleftharpoons}} R'L$$

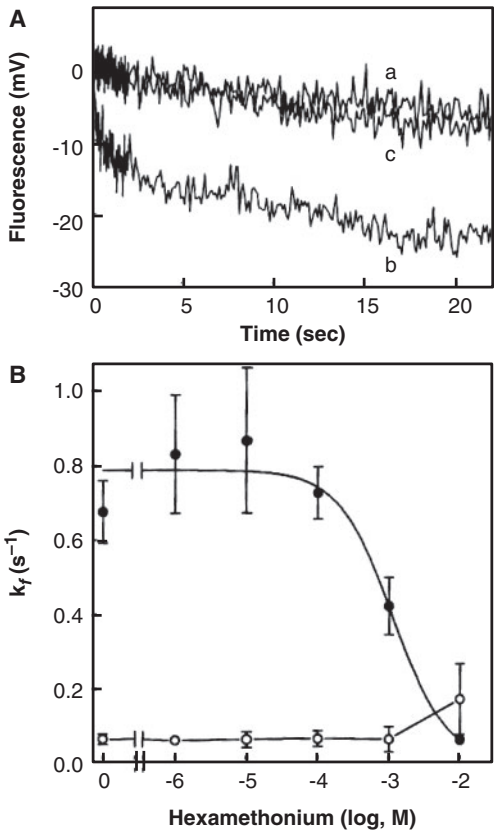

Fig. 1 Agonist-specific effects of intrinsic fluorescence changes. (A) Representative traces of intrinsic fluorescence changes upon rapid mixing of membrane preparations with or without α-BTx pretreatment (~40 min) and *Torpedo* Ringers in the absence or presence of Carb. The final α-BTx concentration was 30 nM. *Traces*: (a) Membrane fragments alone (control). (b) One hundred micromolar Carb. The parameter values obtained from the fit to the two exponential model equations were $A_f = 9.30$ mV, $k_f = 1.81\ s^{-1}$, $A_s = 15.1$ mV, $k_s = 0.047\ s^{-1}$. (c) 100 μM Carb with α-BTx-treated membrane fragments. (B) Concentration dependence of apparent rates (k_f) for hexamethonium alone (open circle) or in the presence of 100 μM Carb (filled circle). For filled circles, each rate was an average of at least five data (mean ± SD). The line was drawn assuming the following sigmoidal model: rate (s^{-1}) $= k_0 + (k_{max} - k_0)/[1 + (10^{\log[L]}/10^{\log IC_{50}})^n]$, where k_0 is the minimum rate, k_{max} is the maximum rate, [*L*] is the concentration of a ligand (*i.e.* hexamethonium), IC_{50} is the half-maximal inhibitory constant, and *n* is the Hill coefficient. The parameter values were as follows: $k_0 = 0.006\ s^{-1}$, $k_{max} = 0.79\ s^{-1}$, $IC_{50} = 1.11$ mM and $n = 1.15$. For open circles, each rate (mean ± SD) was an average of at least four data.

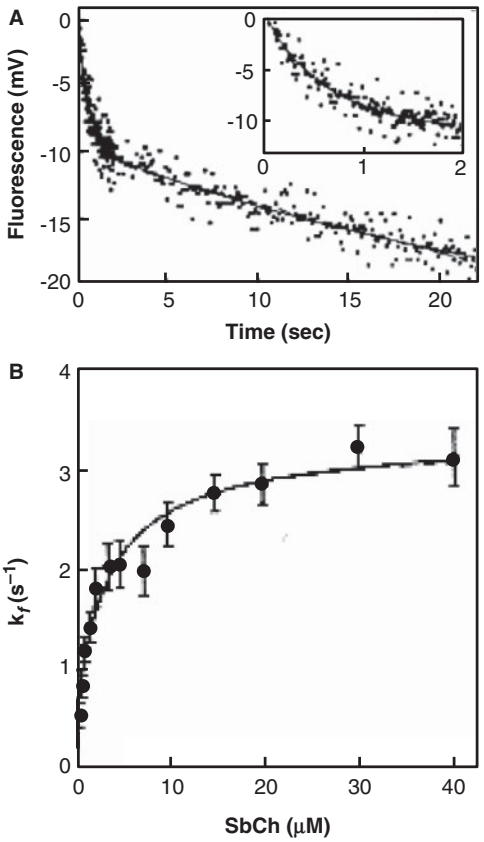

Fig. 2 Intrinsic fluorescence kinetics of suberyldicholine. (A) A trace of intrinsic fluorescence change induced by 7.5 μM SbCh (shown in dots for clarity) was fitted with the two exponential model equation (solid line; $A_f = 9.55$ mV, $k_f = 1.83\ s^{-1}$, $A_s = 11.6$ mV and $k_s = 0.041\ s^{-1}$) and the single exponential equation (dashed line; $A_f = 9.77$ mV, $k_f = 1.52\ s^{-1}$). The dashed line is overlapping with the solid line almost completely. *Inset*: the trace was expanded for clarity and to show no significant difference in data fitting between the two equations. (B) Concentration dependence of the apparent fast rates (k_f) for SbCh. Each date point represents $n = 3$ (mean ± SEM). The apparent slow rates (k_s) were mostly undetected. The solid line shows a sequential model (Scheme I) fitting with Eq. (*1*). The parameter values were $K_1 = 3.03$ μM, $k_2 = 3.06\ s^{-1}$ and $k_{-2} = 0.21\ s^{-1}$.

Table I. Parameters of Scheme I for agonist-induced intrinsic fluorescence kinetics

Parameter	Carb	ACh	SbCh
K_1 (μM)	133	5.14	3.03
k_2 (s^{-1})	3.16	2.93	3.06
k_{-2} (s^{-1})	0.27	0.29	0.21
K_1K_2 (μM)	12.0	0.51	0.20

In this mechanism, the ligand L rapidly complexes with the receptor R forming a ligand–receptor complex RL with an equilibrium binding constant K_1. RL then isomerizes to R′L with a forward rate constant k_2. The receptor in the R′L conformation may slowly convert to the RL form with a backward rate constant k_{-2}. The relaxation rate equation describing this mechanism is:

$$\tau_f^{-1} = \frac{k_2[L]}{K_1 + [L]} + k_{-2}. \quad (1)$$

An iterative procedure of non-linear regression was used to fit concentration–rate curves of the fast phase to Eq. (1) using InPlot4 (GraphPad, Inc.) with no assumption for any parameters (Fig. 2B). The parameter values thus obtained are listed in Table I and compared with values for ACh and Carb as controls. The binding constant obtained for SbCh was 3.03 ± 0.76 μM ($n = 3$), comparable to previously reported values (*27*). The forward rate constant was too slow to account for receptor activation; thus the

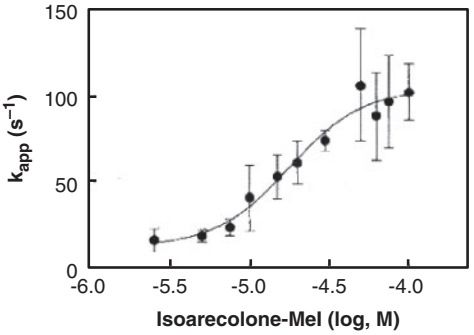

Fig. 3 Stopped-flow Tl^+-flux concentration–rate curve for isoarecolone-MeI. An example of the dose–response curve for receptor activation by isoarecolone-MeI. Curve fitting with the sigmoidal equation gave the following parameter values: $K_{act} = 18.0\,\mu M$, $k_{max} = 105\,s^{-1}$ and $n_H' = 1.84$. The apparent rate for 0.5 mM Carb for this particular membrane preparation was $41.5 \pm 14.0\,s^{-1}$. Error bars are standard errors of the mean (SEM) for multiple data points ($n > 3$) at each concentration used.

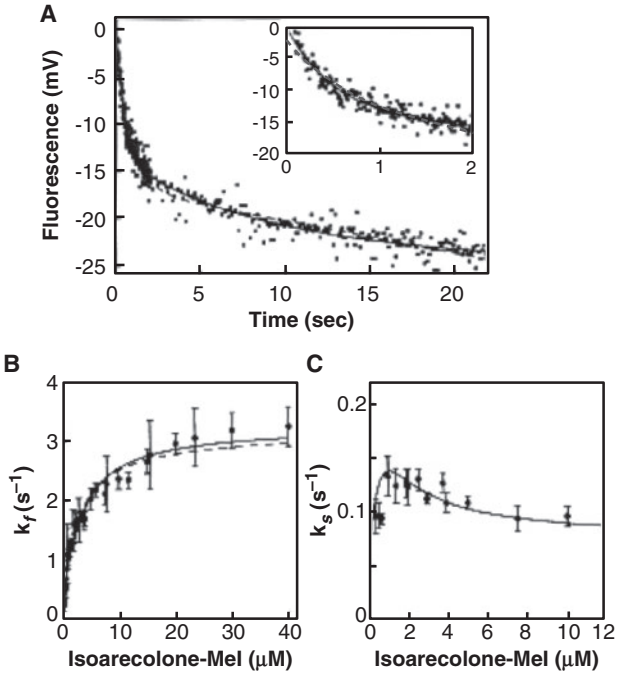

Fig. 4 Intrinsic fluorescence kinetics of isoarecolone-MeI. (A) A trace of intrinsic fluorescence change induced by 5 μM isoarecolone-MeI was fitted with the two exponential model equations (solid line; $A_f = 13.4$ mV, $k_f = 1.99\,s^{-1}$, $A_s = 9.1$ mV and $k_s = 0.135\,s^{-1}$) and the single exponential equation (dashed line; $A_f = 14.7$ mV, $k_f = 1.12\,s^{-1}$). *Inset*: the trace was expanded to show a significant deviation from the single exponential model. (B and C) Concentration dependence of the apparent fast and slow rates for isoarecolone-MeI. Each date point represents $n = 4$ (mean ± SEM). The solid lines show a branching model (Scheme II) fitting with Eq. (*2*) for the fast phase and with Eq. (*3*) for the slow phase.

intrinsic fluorescence changes are likely monitoring conformational transitions of the receptor to a high affinity or desensitized state. The overall effective dissociation constant (K_d) can be calculated using the equation: $K_d = K_1K_2/(1 + K_2)$. The estimated values for ACh, Carb (determined for comparison), and SbCh were 0.46, 11.0 and 0.19 μM, respectively, which are at least 10-fold higher than the equilibrium dissociation constants of desensitized receptors (~10 nM for ACh and SbCh, ~0.1 μM for Carb), indicating that this mechanism does not fully account for conformational transitions of the receptor to the high affinity or desensitized state and may possibly involve a mute step(s) (see Discussion section).

Tl^+-flux response studies using isoarecolone-MeI

We then examined the interaction between isoarecolone-MeI and the nAChR. We first determined the properties of receptor activation by the semirigid ligand using Tl^+-flux stopped-flow spectrofluorimetry and found that isoarecolone-MeI activated the nAChR with a dissociation (activation) constant of 32.0 ± 8.4 μM and Hill coefficient of 1.4 ± 0.2 (mean ± standard error; $n = 3$; Fig. 3). The value of activation constant was approximately 3-fold lower than that of ACh (87.0 μM).

Concentration-dependent effects of isoarecolone-MeI on intrinsic fluorescence changes

We then examined intrinsic fluorescence changes induced by this agonist. In addition to fast rates that were similar to those for the agonists discussed above, kinetic traces induced by isoarecolone-MeI contained a second phase with slow rates that were within the criteria for the sum of two exponential equations (Fig. 4). The apparent slow rates increased at low concentrations and then decreased at high concentrations. This phenomenon can be described by the following branched mechanism:

Scheme II

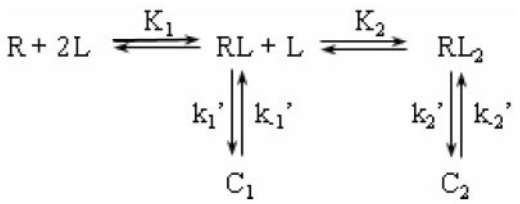

This scheme was initially proposed from kinetic studies using ethidium bromide, an extrinsic fluorescent probe, to monitor ligand-induced conformational transitions of the receptor induced by Carb (*19*, *37*). Studies with 5-(iodoacetamido)salicylate (IAS)-labelled nAChR confirmed this scheme and further developed it to include a fast isomerization step prior to the isomerization to C_1 (*24*). Using ethidium bromide, Carb-induced fluorescent changes showed (at least) two concentration dependent kinetic phases; one phase being a hyperbolic fast phase, the other being an increase followed by a decrease in rate for a slow phase. In this scheme, two ligands rapidly pre-equilibrate before each form of ligand-bound

Table II. Parameters of Scheme II for isoarecolone-MeI-induced intrinsic fluorescence kinetics

Parameter	Isoarecolone-MeI
K_1 (μM)	1.5
K_2 (μM)	3.0
k_1' (s^{-1})	0.26
k_{-1}' (s^{-1})	0.072
k_2' (s^{-1})	2.62
k_{-2}' (s^{-1})	0.60
K_1K_1' (μM)	0.42
K_2K_2'/K_1' (μM)	2.46

receptor (RL and RL_2) isomerizes to C_1 and C_2, respectively. A high concentration of L favours the formation of RL_2, which is then converted to C_2 with a relatively fast rate. At a low concentration of L, mono-liganded receptor (RL) slowly changes its conformation to C_1. This phase disappears as the di-liganded form of the receptor–ligand complex predominates when the ligand concentration is increased; thus resulting in the increase-then-decrease slow rates in a concentration dependent manner. The relaxation rate equations describing Scheme II are for the fast phase (step 2′):

$$\tau_2^{-1} = k_2'\left(\frac{[L]^2/K_1K_2}{1+[L]/K_1+[L]^2/K_1K_2}\right) + k_{-2}' \qquad (2)$$

and for the slow phase (step 1′),

$$\tau_1^{-1} = k_1'\left(\frac{[L]/K_1}{1+[L]/K_1+[L]^2/K_1K_2K_2'}\right) + k_{-1}'. \qquad (3)$$

These two equations were used to fit the concentration–rate curves for the two phases (Fig. 4B and C, Table II). A good fit was obtained with $K_1 = 1.5\,\mu M$, $K_2 = 3.0\,\mu M$, $k_2' = 2.62\,s^{-1}$, and $k_{-2}' = 0.60\,s^{-1}$ for the fast phase and $k_1' = 0.26\,s^{-1}$ and $k_{-1}' = 0.072\,s^{-1}$ for the slow phase using the values of K_1, K_2 and K_2' ($=k_{-2}'/k_2'$). The rate constants for the fast phase (step 2′) were in good agreement with the values obtained for the kinetic studies using ethidium bromide (*19*, see also *24*). The rate constants for the slow phase (step 1′), however, were an order of magnitude greater than those from the ethidium monitored kinetics. This may be a function of the ligands used in the two studies, *i.e.* Carb in the ethidium studies versus isoarecolone-MeI used here.

Discussion

The observed concentration dependent changes in intrinsic fluorescence were due to the nAChR and specific to agonists since (i) α-BTx preincubation of the membrane preparation abolished Carb-induced fluorescence quenching, (ii) an antagonist, hexamethonium, did not induce fluorescence changes, and (iii) Carb-induced fluorescence quenching was blocked by hexamethonium in a concentration dependent manner. The absence of hexamethonium-induced kinetics was consistent with previous studies (*19*), where the antagonist exhibited only weak concentration dependency in its kinetics monitored using the extrinsic fluorescent probe ethidium bromide. In contrast, agonist-induced kinetics contained at least one phase with a relatively fast rate ($t_{1/2} = 0.2$–$1.2\,s$). Although some slow rates were also detected with ACh, Carb and SbCh, consistent slow rates were only obtained for the semirigid agonist isoarecolone-MeI.

Previously, we have demonstrated that another semirigid agonist, arecolone-methioide, also induced slow rates consistently, but the kinetic model that fits the show rates was a sequential mechanism and thus was distinct from the branched mechanism observed here for isoarecolone-MeI (*38*). Agonists such as ACh and Carb are flexible ligands that adapt their structures at the agonist binding sites as the ligand–receptor complex changes its conformation (*39*). Such structural changes will be restricted in semirigid agonists, which possess a dihydropyridine ring between the acetyl group and the quaternary amine. Thus, the consistent detection of the slow rates observed in this and previous work might be due to the structural rigidity of semirigid agonists. Meanwhile, different kinetics of the slow rates observed for the two semirigid agonists that structurally differ only at the position of the acetyl group (position 3 for arecolone-MeI versus position 4 for isoarecolone-MeI in the dihydropyridine ring) suggests that the agonist binding sites of nAChRs are highly sensitive to ligand structure for inducing different conformations of nAChR. This is consistent with the observations that the determinants of ligand recognition in the agonist binding sites are diverse and that specific recognition of various ligand structures by different amino acids determines ligand activity (*11*, *40*).

For ACh, Carb and SbCh, the observed kinetics was consistent with the simple sequential mechanism (Scheme I) in agreement with previous reports (*27*, *28*). However, our results indicate that the final conformational state does not appear to represent the high affinity desensitized state in contrast to these authors' interpretation. The pathway to the final state (R′L in Scheme I) had an overall dissociation constant that was at least 10 times higher than the equilibrium dissociation constants of these agonists, indicating that the scheme does not entirely describe the desensitization process described originally by Katz and Thesleff (*16*). One possible interpretation of this is that the intrinsic fluorescence kinetics monitors the formation of a distinct state of receptor conformation because the slow phase is simply mute for these agonists (*i.e.* ACh, Carb and SbCh) using intrinsic fluorescence. Alternatively, the final conformational state observed here may be an intermediate in the pathway to the desensitized state and the scheme can be considered to be only partial in terms of the desensitization process.

The fluorescence change previously attributed to the initial binding step of SbCh (*27*) was not detected here. In addition, the rate constants k_2 and k_{-2} for ACh and Carb were an order of magnitude larger than the values obtained in these previous studies. These discrepancies may be due to the difference in membrane

preparations and in the improvement in signal detection by improved instrumentation. It was noted that the k_2 of $\sim 3\,s^{-1}$ was an order of magnitude greater than the rate of slow desensitization obtained using agonist binding and ion-flux studies (*20*, *41*, *42*) but was consistent with the rate constants for fast desensitization reported using ion flux studies (*i.e.* $2–8\,s^{-1}$) (*29*, *41*, *43*), suggesting that the fast phase detected using the intrinsic fluorescence changes describes the formation of a fast desensitized state but not of a slow desensitized state.

In contrast to ACh, Carb and SbCh, isoarecolone-MeI allowed routine detection of an additional phase with a slow rate and thus contained two kinetic phases. Scheme II accounts for the binding of two agonists to each receptor molecule. This mechanism suggests that one molecule of isoarecolone-MeI binds to one of the two sites and induces a slow conformational transition to C_1. At high ligand concentrations, a second ligand induces the formation of C_2 with a faster rate. An effective dissociation constant for second ligand binding can be approximated by K_{eff} $(\mu M) = K_2K_2'/K_1'$, giving a value of 2.46 μM. This value is much greater than the value for the formation of C_1, which can be estimated to be $K_1K_1' = 0.42\,\mu M$, suggesting a significant difference in the affinities for the two forms of the receptor.

The forward rate constants of the slow phase for isoarecolone-MeI were in the range of $0.08–0.15\,s^{-1}$ ($t_{1/2}$ ≈4.5–9 s) (*cf.* Fig. 4C). The rate constants for the slow phase (step 1′) were an order of magnitude higher than the values obtained for agonists with ethidium bromide. It was suggested from the ethidium kinetics that $R \rightarrow RL \rightarrow C_1$ pathway describes the slow desensitization process to the high affinity equilibrium state described previously (*16*) since the value of K_1K_1' obtained for Carb (*i.e.* 0.10 μM) was in good agreement with the equilibrium dissociation constant of the agonist from direct binding studies (*19*). The overall dissociation constant of C_1 formation for isoarecolone-MeI ($K_1K_1' = 0.42\,\mu M$) appears to be higher than an expected dissociation constant for this agonist obtained from equilibrium displacement studies with [^{3}H]-Carb (0.097 μM, Kawai and Raftery, unpublished observations). Therefore C_1 may be an intermediate conformation toward the high affinity desensitized state. Since the slow rates were consistent with those from the kinetic studies with IAS (*24*), the isomerization step prior to C_1 formation observed with IAS may be mute in the intrinsic fluorescence kinetics. Thus, the $R \rightarrow RL \rightarrow C_1$ pathway described here may be a partial description of the slow desensitization process toward the high affinity state. Overall, the intrinsic fluorescence kinetic mechanism (Scheme II) was consistent with that proposed for ethidium- (*19*) and IAS-monitored (*24*) conformational transitions. Although a particular kinetic step(s) may be unobservable depending on the fluorescence probe used, the consistency of observed kinetic mechanisms using these various types of fluorescent probes strongly supports the validity of the proposed mechanism of receptor conformational transitions.

Acknowledgements

We thank Dr Susan M.J. Dunn for helpful discussions. We are grateful to David K. Okita for membrane preparations.

Funding

This work was supported by the National Institute on Drug Abuse (NIDA) Program Project Grant DA08131 (M.A.R.).

Conflict of interest

None declared.

References

1. Raftery, M.A., Hunkapiller, M.W., Strader, C.D., and Hood, L.E. (1980) Acetylcholine receptor: complex of homologous subunits. *Science* **208**, 1454–1456
2. Noda, M., Takahashi, H., Tanabe, T., Toyosato, M., Kikyotani, S., Furutani, Y., Hirose, T., Takashima, H., Inayama, S., Miyata, T., and Numa, S. (1983) Structural homology of *Torpedo californica* acetylcholine receptor subunits. *Nature* **302**, 528–532
3. Corringer, P.J., Le Novere, N., and Changeux, J.P. (2000) Nicotinic receptors at the amino acid level. *Annu. Rev. Pharmacol. Toxicol.* **40**, 431–458
4. Arias, H.R. (2000) Localization of agonist and competitive antagonist binding sites on nicotinic acetylcholine receptors. *Neurochem. Int.* **36**, 595–645
5. Sine, S.M. (2002) The nicotinic receptor ligand binding domain. *J. Neurobiol.* **53**, 431–446
6. Karlin, A. (2002) Emerging structure of the nicotinic acetylcholine receptors. *Nat. Rev. Neurosci.* **3**, 102–114
7. Bode, J., Moody, T., Schimerlik, M., and Raftery, M. (1979) Uses of fluorescent cholinergic analogues to study binding sites for cholinergic ligands in *Torpedo californica* acetylcholine receptor. *Biochemistry* **18**, 1855–1861
8. Watters, D., and Maelicke, A. (1983) Organization of ligand binding sites at the acetylcholine receptor: a study with monoclonal antibodies. *Biochemistry* **22**, 1811–1819
9. Dunn, S.M., and Raftery, M.A. (1997) Agonist binding to the *Torpedo* acetylcholine receptor. 1. Complexities revealed by dissociation kinetics. *Biochemistry* **36**, 3846–3853
10. Dunn, S.M.J., and Raftery, M.A. (1997) Agonist binding to the *Torpedo* acetylcholine receptor. 2. Complexities revealed by association kinetics. *Biochemistry* **36**, 3854–3863
11. Carter, C.R., Cao, L., Kawai, H., Smith, P.A., Dryden, W.F., Raftery, M.A., and Dunn, S.M. (2007) Chain length dependence of the interactions of bisquaternary ligands with the *Torpedo* nicotinic acetylcholine receptor. *Biochem. Pharmacol.* **73**, 417–426
12. Kawai, H., Dunn, S.M., and Raftery, M.A. (2008) Epibatidine binds to four sites on the *Torpedo* nicotinic acetylcholine receptor. *Biochem. Biophys. Res. Commun.* **366**, 834–839
13. Dunn, S.M., and Raftery, M.A. (1982) Activation and desensitization of *Torpedo* acetylcholine receptor: evidence for separate binding sites. *Proc. Natl. Acad. Sci. USA* **79**, 6757–6761
14. Dunn, S.M., and Raftery, M.A. (1982) Multiple binding sites for agonists on *Torpedo californica* acetylcholine receptor. *Biochemistry* **21**, 6264–6272
15. Dunn, S.M., and Raftery, M.A. (1993) Cholinergic binding sites on the pentameric acetylcholine receptor of Torpedo californica. *Biochemistry* **32**, 8608–8615

16. Katz, B., and Thesleff, S. (1957) A study of the desensitization produced by acetylcholine at the motor end-plate. *J. Physiol. (London)* **138**, 63–80
17. Grunhagen, H.-H., and Changeux, J.-P. (1976) Studies on the electrogenic action of acetylcholine with *Torpedo marmorata* electric organ. V. Qualitative correlation between pharmacological effects and equilibration processes of the cholinergic receptor protein as revealed by the structural probe quinacrine. *J. Mol. Biol.* **106**, 517–535
18. Grunhagen, H.-H., Iwatsubo, M., and Changeux, J.-P. (1977) Fast kinetic studies on the interaction of cholinergic agonists with the membrane-bound acetylcholine receptor from *Torpedo marmorata* as revealed by quinacrine fluorescence. *Eur. J. Biochem.* **80**, 225–242
19. Quast, U., Schimerlik, M.I., and Raftery, M.A. (1979) Ligand-induced changes in membrane-bound acetylcholine receptor observed by ethidium fluorescence. 2. Stopped-flow studies with agonists and antagonists. *Biochemistry* **18**, 1891–1901
20. Heidmann, T., and Changeux, J.P. (1979) Fast kinetic studies on the interaction of a fluorescent agonist with the membrane-bound acetylcholine receptor from *Torpedo marmorata*. *Eur. J. Biochem.* **94**, 255–279
21. Heidmann, T., and Changeux, J.P. (1980) Interaction of a fluorescent agonist with the membrane-bound acetylcholine receptor from *Torpedo marmorata* in the millisecond time range: resolution of an "intermediate" conformational transition and evidence for positive cooperative effects. *Biochem. Biophys. Res. Commun.* **97**, 889–896
22. Prinz, H., and Maelicke, A. (1983) Interaction of cholinergic ligands with the purified acetylcholine receptor protein. II. Kinetic studies. *J. Biol. Chem.* **258**, 10273–10282
23. Prinz, H., and Maelicke, A. (1992) Ligand binding to the membrane-bound acetylcholine receptor from *Torpedo marmorata*: a complete mathematical analysis. *Biochemistry* **31**, 6728–6738
24. Dunn, S.M., Blanchard, S.G., and Raftery, M.A. (1980) Kinetics of carbamylcholine binding to membrane-bound acetylcholine receptor monitored by fluorescence changes of a covalently bound probe. *Biochemistry* **19**, 5645–5652
25. Eldefrawi, M.E., Eldefrawi, A.T., and Wilson, D.B. (1975) Tryptophan and cystein residues of the acetylcholine receptors of *Torpedo* species. Relationship to binding of cholinergic ligands. *Biochemistry* **14**, 4304–4310
26. Barrantes, F.J. (1976) Intrinsic fluorescence of the membrane-bound acetylcholine receptor: its quenching by suberyldicholine. *Biochem. Biophys. Res. Commun.* **72**, 479–488
27. Barrantes, F.J. (1978) Agonist-mediated changes of the acetylcholine receptor in its membrane environment. *J. Mol. Biol.* **124**, 1–26
28. Bonner, R., Barrantes, F.J., and Jovin, T.M. (1976) Kinetics of agonist-induced intrinsic fluorescence changes in membrane-bound acetylcholine receptor. *Nature* **263**, 429–431
29. Waters, J.A., Spivak, C.E., Hermsmeier, M., Yadav, J.S., Liang, R.F., and Gund, T.M. (1988) Synthesis, pharmacology, and molecular modeling studies of semirigid, nicotinic agonists. *J. Med. Chem.* **31**, 545–554
30. Spivak, C.E., Gund, T.M., Liang, R.F., and Waters, J.A. (1986) Structural and electronic requirements for potent agonists at a nicotinic receptor. *Eur. J. Pharmacol.* **120**, 127–131
31. Spivak, C.E., Waters, J.A., and Aronstam, R.S. (1989) Binding of semirigid nicotinic agonists to nicotinic and muscarinic receptors. *Mol. Pharmacol.* **36**, 177–184
32. Neubig, R.R., Krodel, E.K., Boyd, N.D., and Cohen, J.B. (1979) Acetylcholine and local anesthetic binding to Torpedo nicotinic postsynaptic membranes after removal of nonreceptor peptides. *Proc. Natl. Acad. Sci. USA* **76**, 690–694
33. Moore, H.P., Hartig, P.R., Wu, W.C., and Raftery, M.A. (1979) Rapid cation flux from *Torpedo californica* membrane vesicles: comparison of acetylcholine receptor enriched and selectively extracted preparations. *Biochem. Biophys. Res. Commun.* **88**, 735–743
34. Elliott, J., Blanchard, S.G., Wu, W., Miller, J., Strader, C.D., Hartig, P., Moore, H.-P., Racs, J., and Raftery, M.A. (1980) Purification of *Torpedo californica* post-synaptic membranes and fractionation of their constituent proteins. *Biochem. J.* **185**, 667–677
35. Schmidt, J., and Raftery, M.A. (1973) A simple assay for the study of solubilized acetylcholine receptors. *Anal. Biochem.* **52**, 349–354
36. Moore, H.-P.H., and Raftery, M.A. (1980) Direct spectroscopic studies of cation translocation by *Torpedo* acetylcholine receptor on a time scale of physiological relevance. *Proc. Natl Acad. Sci. USA* **77**, 4509–4513
37. Quast, U., Schimerlik, M.I., and Raftery, M.A. (1978) Stopped flow kinetics of carbamylcholine binding to membrane bound acetylcholine receptor. *Biochem. Biophys. Res. Commun.* **81**, 955–964
38. Kawai, H., Cao, L., Dunn, S.M., Dryden, W.F., and Raftery, M.A. (2000) Interaction of a semirigid agonist with *Torpedo* acetylcholine receptor. *Biochemistry* **39**, 3867–3876
39. Behling, R.W., Yamane, T., Navon, G., and Jelinski, L.W. (1988) Conformation of acetylcholine bound to the nicotinic acetylcholine receptor. *Proc. Natl Acad. Sci. USA* **85**, 6721–6725
40. Hansen, S.B., Sulzenbacher, G., Huxford, T., Marchot, P., Taylor, P., and Bourne, Y. (2006) Structures of Aplysia AChBP complexes with nicotinic agonists and antagonists reveal distinctive binding interfaces and conformations. *EMBO J.* **24**, 3635–3646
41. Walker, J.W., Takeyasu, K., and McNamee, M.G. (1982) Activation and inactivation kinetics of *Torpedo californica* acetylcholine receptor in reconstituted membranes. *Biochemistry* **21**, 5384–5389
42. Neubig, R.R., Boyd, N.D., and Cohen, J.B. (1982) Conformations of *Torpedo* acetylcholine receptor associated with ion transport and desensitization. *Biochemistry* **21**, 3460–3467
43. Takeyasu, K., Shiono, S., Udganokar, J.B., Fujita, N., and Hess, G.P. (1986) Acetylcholine receptor: characterization of the voltage-dependent regulatory (inhibitory) site for acetylcholine in membrane vesicles from *Torpedo californica* electroplax. *Biochemistry* **25**, 1770–1776